Applied Physics Letters

Electric-field-induced optical hysteresis in single-layer WSe_2

Cite as: Appl. Phys. Lett. **115**, 161103 (2019); https://doi.org/10.1063/1.5123514
Submitted: 07 August 2019 . Accepted: 29 September 2019 . Published Online: 14 October 2019

Zheng Sun, Jonathan Beaumariage, Ke Xu, Jierui Liang, Shaocong Hou, Stephen R. Forrest, Susan K. Fullerton-Shirey, and David W. Snoke

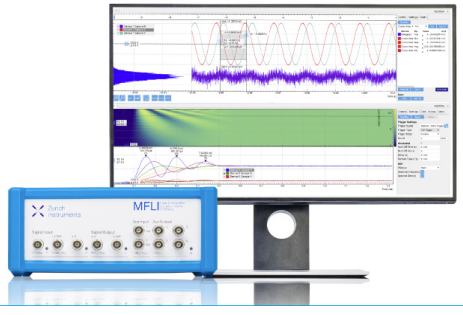

Applied Physics Letters ARTICLE scitation.org/journal/apl

Electric-field-induced optical hysteresis in single-layer WSe_2

Cite as: Appl. Phys. Lett. **115**, 161103 (2019); doi: 10.1063/1.5123514
Submitted: 7 August 2019 · Accepted: 29 September 2019 ·
Published Online: 14 October 2019

Zheng Sun,[1,a),b)] Jonathan Beaumariage,[1,a)] Ke Xu,[2] Jierui Liang,[2] Shaocong Hou,[3] Stephen R. Forrest,[3] Susan K. Fullerton-Shirey,[2] and David W. Snoke[1,b)]

AFFILIATIONS

[1]Department of Physics and Astronomy, University of Pittsburgh, Pittsburgh, Pennsylvania 15260, USA
[2]Department of Chemical and Petroleum Engineering, University of Pittsburgh, Pittsburgh, Pennsylvania 15260, USA
[3]Department of Electric Engineering and Computer Science, University of Michigan, Ann Arbor, Michigan 48109, USA

[a)]**Contributions:** Z. Sun and J. Beaumariage contributed equally to this work.
[b)]**Authors to whom correspondence should be addressed:** zhengsun@pitt.edu and snoke@pitt.edu

ABSTRACT

We demonstrate that the exciton energy of a monolayer of tungsten diselenide on an SiO_2/Si substrate can be tuned by an applied in-plane electric field for two samples with different dielectric capping materials. The exciton energy can be either red- or blue-shifted by up to 20 meV based on the polarity of the applied electric field. We argue that a piezoelectric effect creates a large internal electric field, which is either partially aligned or partially antialigned with the external electric field. Additionally, optical hysteresis is observed on cycling of the external electric field due to trapped charges.

The many possible configurations of van der Waals heterostructures make transition-metal dichalcogenides (TMDs) promising for next-generation electronic and optoelectronic devices.[1–4] A monolayer of TMD with the form MX_2 (e.g., M = Mo or W; X = S or Se) is a direct bandgap semiconductor.[5,6] TMD monolayers also have extraordinarily strong optical oscillator strengths and large exciton binding energies (0.3–0.5 eV).[7,8]

Strong light-matter coupling leads to polariton states, as reported in optical microcavities at both room and cryogenic temperatures.[9–13] To the best of our knowledge, however, optical nonlinearities and spontaneous coherence have not yet been observed in these systems. These phenomena require resonance between the cavity photon energy and the TMD exciton energies, either via tuning of the microcavity thickness or via tuning of the exciton energy by an electromagnetic field or other external means. Control of the microcavity thickness can be obtained by growing TMD layers over a wide area using chemical vapor deposition (CVD) or molecular beam epitaxy (MBE), and then a gradient, or wedge, of the microcavity spacer thickness can be used to tune the cavity photon energy, as done in III–V polariton structures at a low temperature.[14] Although many research groups are investigating wide-area growth of TMD layers, to date, the optical quality of these samples is still poor in comparison to small-area samples created via exfoliation. Therefore, various methods to tune the exciton energy of exfoliated samples may provide an alternative route. Prior work has shown that the bandgap of TMDs can be tuned by strain, either by bending a soft substrate[15–17] or applying an external force through a stressor.[18] Unfortunately, neither of these techniques can be easily applied in practical devices. Vertical electric field tuning has been used with spatially indirect excitons in bilayer structures,[19,20] but indirect excitons have a much lower oscillator strength, making them less useful as candidates for strong light-matter coupling. We therefore focus on shifting the energy of the excitons in monolayers.

Here, we measure the Stark shift predicted in 2D TMD materials due to an applied in-plane electric field.[21] This method has been used previously with TMD layers, including using an electric field to modify the exciton-polariton coupling strength in a microcavity.[22] However, a systematic investigation of tuning the exciton energy in monolayer TMDs has not yet been reported. In this paper, we report a systematic experimental study of the exciton energy in monolayer tungsten diselenide (WSe_2) under continuous tuning by an in-plane electric field. To avoid arcing between contacts (which occurs around 10 kV/cm), thin layers of the dielectric materials hBN and SiO_2 were used as a protective capping layer of the TMD flakes. This approach can be extended to other TMDs with optical bandgaps.

Isolated monolayer flakes of WSe_2 (bulk crystals purchased from 2D semiconductors) with a typical size of $5 \times 15\ \mu m^2$ were mechanically exfoliated and transferred to the surfaces of two separate p-doped silicon substrates with 90 nm of SiO_2 (purchased from the Graphene Supermarket). The transfer was performed in air. The thicknesses of the flakes were characterized by micro-Raman spectroscopy, in which we observe the main typical lattice vibration mode A_g^1 ($252\ cm^{-1}$) (supplementary material, Sec. 1), consistent with the reported values for a monolayer.[24] Two contacts were written on top of each flake via e-beam lithography, to give an electric field parallel to the surface; this was followed by e-beam deposition of Ti/Au 3/100 nm. The metals were deposited at a pressure of 10^{-6} Torr. Device 1 was capped with a 15-nm film of exfoliated hBN (bulk crystal purchased from 2D semiconductors), and device 2 was capped with 90 nm of SiO_2 grown via plasma-enhanced vapor deposition (PECVD). The contacts were then wirebonded. In device 1, the wirebonds were in direct contact with the gold pad, while in device 2, the wirebonds were separated from the gold pads by 90 nm of SiO_2. Figure 1(a) illustrates the design of each device.

The photoluminescence (PL) spectra of monolayer WSe_2 were measured by nonresonantly pumping the devices at room temperature with a 632-nm HeNe laser with a spot size of $5\ \mu m$ at normal incidence through a microscope objective while the substrate was grounded. The PL spectra were collected by the same microscope objective and directed towards a spectrometer equipped with a charge coupled device (CCD) camera. The reflected He-Ne laser light was removed using several long-pass filters. Even though some of the pump laser overfills the sample, the monolayer region is responsible for the vast majority of the signal due to the efficient optical transition at the K point in the Brillouin zone. The PL spectra of the capped samples are shown in Fig. 1(b). The measurement in Fig. 1(b) (blue curve) was performed on uncapped samples. Before capping, both samples exhibit a main peak due to exciton A (ex_A) centered at 1.668 eV with an FWHM of 65 meV. After capping device 1 with hBN, the ex_A peak significantly narrows and red shifts, resulting in an FWHM of 37 meV centered at 1.630 eV, while the measured PL intensity does not significantly change. After capping device 2 with SiO_2, the linewidth broadens to 75 meV and further red shifts to 1.597 eV, with the intensity of the PL dropping by a factor of 4500 which was fit by the Lorentz function. The red shift of TMD exciton energies due to the presence of capping and substrate materials has been previously observed and was attributed to the change of the dielectric environment, resulting in a change of both the exciton binding energy and a shift of the bandgap.[8,25]

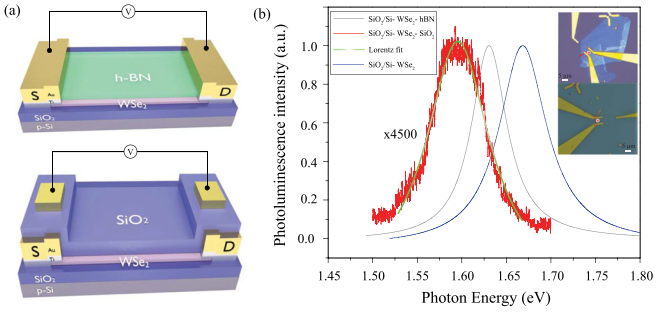

FIG. 1. (a) Schematics of two samples capped with (top, device 1) a 15 nm film of exfoliated hBN and (bottom, device 2) 90 nm of SiO_2 grown by PECVD. Ti/Au source/drain contacts were on the WSe_2 monolayer flake prior to the addition of the capping layer. (b) Typical photoluminescence emission spectra of the WSe_2 excitons in the uncapped sample (blue curve), the sample capped with hBN (gray curve), and the sample capped with SiO_2 (red curve) with the Lorentz fit (green curve). The insets are the optical microscope images of the devices with hBN and SiO_2 capping, respectively. Capping the samples red shifts the excitons. Note that the sample capped with SiO_2 shifts the furthest, in agreement with another study.[23]

Electrical characterization without optical pumping was carried out using a Keysight B1500A semiconductor parameter analyzer in a Lakeshore cryogenic vacuum probe station (CRX-VF) at a pressure of 2×10^{-6} Torr. Figure 2 shows the electrical response of the source-drain current as a function of the source-drain voltage for device 1. The sharp rise in current at around 10 V for both positive and negative voltages indicates that the current is crossing a tunneling barrier. The hysteresis observed here has been reported previously and was attributed to the behavior to the trapping states induced by absorbed water molecules on the TMD surface.[26] The authors of that work also noted that the photosensitivity of the TMDs significantly increased the hysteresis when it was exposed to white illumination, which also indicates the presence of trapped charge excited by high-energy photons.

Device 1 was wire-bonded to a chip carrier, which in turn, was connected to a Keithley 2326B. Keeping the substrate grounded, the source-drain voltage was ramped from 0 to 40 V, then down to −40 V, and back to 0 V, all at 1 V increments. After cycling several times, the PL was collected as described above, and the center of the dominant peak position was recorded and plotted vs the bias voltage, as shown in Fig. 2(b).

As seen in Fig. 2, hysteresis is observed in both the electrical current and the exciton energy in the optical signal. The optical signal shows two additional features. The first is that the energy of the exciton at 0 V is permanently blue-shifted relative to its value (from 1.63 to 1.644 eV) before the voltage was applied; thus, the red shift originally induced by the capping layer has been decreased. The second is that we found the Stark shift of the exciton is not always of lower energy, which is unexpected.

The overall red shift of the exciton energy relative to the uncapped sample is likely due to the internal electric field that arises when the capping layer is added, which we attribute to the result of piezoelectric effects from the strain between the TMD and the cap. This internal electric field is larger than the external electric field, which either partially cancels or augments it. The permanent, slight blue shift after voltage cycling is presumably the result of the applied electric field relaxing the strains, and hence the internal electric field.

The Stark shift is predicted to be quadratic with the total electric field and is always of lower energy.[21] We can write this as the sum of the internal and external electric fields,

$$\Delta E = \frac{1}{2}\alpha F^2 = \frac{1}{2}\alpha(F_{\text{int}} + F_{\text{ext}})^2, \tag{1}$$

where the energy shift ΔE is given in terms of the polarizability of the excitons α and the electric field strength F. By taking the externally applied electric field as the bias voltage divided by the S/D contact separation distance ($5\ \mu m$), Eq. (1) predicts a quadratic dependence for the data in Fig. 2(b). Because the measured shift is linear with the applied electric field, we conclude that the internal field is much larger than the externally applied field. We approximate the above equation

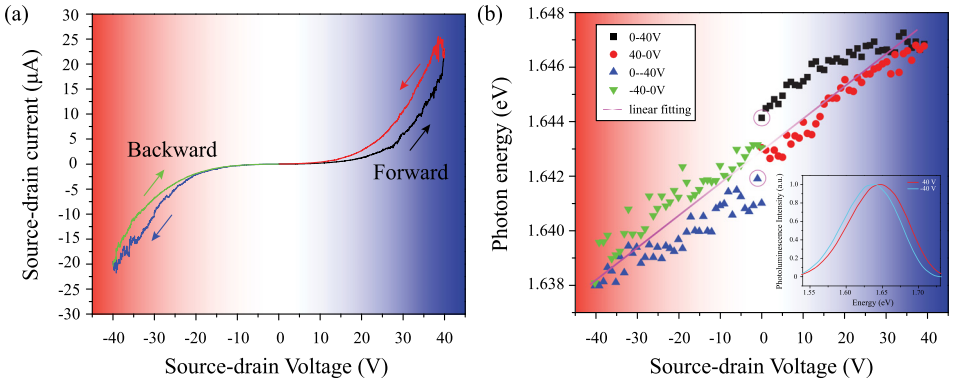

FIG. 2. (a) Source-drain current as a function of the source-drain voltage in device 1; the substrate is set to the ground. Optical pumping was not used while these data were collected; the ramping speed is 20 mV/s. (b) The maximum photon energy of the PL of ex_A as a function of an externally applied source-drain voltage in device 1, after cycling through the voltage loop several times. The exciton energy at 0 applied voltage switches between 1.644 and 1.641 eV based on the location in the loop. Both of these values are between the exciton energies before and after adding the capping layer. The red shift due to capping with hBN was permanently reduced, as found by remeasuring the sample one week later. The inset shows two typical PL spectra under the applied voltages.

to the first order in F_{ext}, and then take the derivative with respect to the external field to compare to the slope of the data in Fig. 2(b),

$$\frac{dE}{dV_{ext}} = \alpha \frac{F_{int}}{d}, \tag{2}$$

where d is the S/D separation distance of 5 μm and $V_{ext} = F_{ext} d$. Fitting our data to a straight line, we find that $\alpha = 5 \times 10^{-5}$ meV cm^2/kV^2, which is reasonably close to the predicted values for other TMD materials.[21] Additionally, we find that the internal electric field is 1220 kV/cm, corresponding to about 0.06% strain for a piezoelectric-constant value of 5 pm/V,[27,28] which is much larger than our externally applied electric field of 80 kV/cm, justifying our approximation above.

When the same measurement was done on device 2, some key differences were observed. In device 2, cycling through the voltage loop did not permanently reduce the initial red shift introduced when the capping layer was added. It has been shown that WSe_2 in contact with SiO_2 experiences a larger surface strain.[23] Thus, we expect that the surface bonds are stronger and so a larger applied electric field would be necessary to relax them. Additionally, we note that the shifting of the PL in the SiO_2-capped sample saturates at an applied voltage of 10 V. The SiO_2 layer between the gold wire bond on the top and the gold contact on the bottom is about 90 nm thick. Given that the applied voltage is 10 V, we see that an electric field of 1.1 MV/cm is plausible in this region, which is near the breakdown limit of SiO_2. It is therefore likely that a small leakage current is present, preventing a larger energy shift and resulting in the observed saturation.

When we attempted to obtain an I–V curve for device 2; we found that the DC was always well below the noise threshold of our equipment. It should be noted that device 2 has two capacitors formed by the layer of SiO_2 between the top metal contacts and the buried metal pads as shown in the lower illustration of Fig. 1(a). By measuring this capacitance (see the supplementary material), we calculated the applied electric field as a function of the source-drain voltage [Fig. 3(b)]. The graph shows a linear relationship with respect to the external voltage, but with the absolute maximum value of 100 kV/cm for positive polarity and 30 kV/cm for negative polarity. From Fig. 3(a), we see the exciton energy changes by 9 meV for negative polarity and by 21 meV for positive polarity. We attribute the asymmetric energy shifts in Fig. 3(a) to the asymmetric behavior of the in-plane electric field in the WSe_2. These polarity-dependent differences are due to the different contact resistances at the two metal/WSe_2 interfaces. It has been reported that the Schottky barrier heights between the metal and WSe_2 can be different on the same device

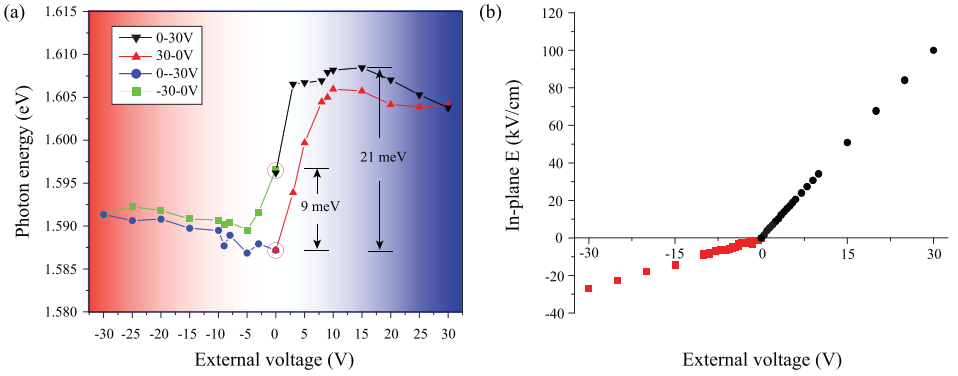

FIG. 3. (a) Photoluminescence of ex_A in device 2, as a function of an externally applied source-drain voltage, after cycling through the voltage loop several times. Unlike device 1, the initial red shift does not change after voltage cycling. The exciton energy at 0 applied voltage switches between 1.586 and 1.597 eV based on the location in the loop. Note that the graph is asymmetric in polarity. (b) The applied electric field in the plane of the WSe_2 flake as a function of the source-drain voltage.

despite using the same contact metal; this is due to the effect of Fermi-level pinning[29,30] or interfacial residue.[31]

Tuning the exciton energy inside TMD monolayers is essential for creating microcavities to study strong light-matter coupling. The in-plane method of applying the electric field demonstrated here lends itself to integration with microcavity devices, because there is no need to dope the mirrors. Here, we have shown that the exciton energy of monolayer WSe_2 can be tuned using an externally applied electric field. About 10 and 20 meV of the total tunable range are demonstrated in hBN- and SiO_2-capped samples, respectively, with the SiO_2 capped sample showing a larger tunability but a reduced PL intensity. The ability to both red and blue shift the exciton energy suggests the presence of an internal electric field, consistent with a piezoelectric effect due to the strain from the capping layer. The hysteresis observed in the voltage-dependent PL is presumably due to trapped charges. Our methods may be extended to tuning the exciton energy of a TMD monolayer inside a microcavity, eventually leading to novel devices for studying strong coupling in TMD systems.

See the supplementary material for the complete study of the capacitor charging measurements and temperature-dependent photoluminescence of a monolayer WSe_2 capped with hBN.

This work was supported by the U.S. Army Research Office under MURI Award No. W911NF-17-1-0312. K.X., J.L., and S.K.F.-S. acknowledge funding from the National Science Foundation, Grant No. 1607935. S.R.F. also acknowledges support from the National Science Foundation, Grant No. 1709163.

REFERENCES

[1]O. Lopez-Sanchez, D. Lembke, M. Kayci, A. Radenovic, and A. Kis, Nat. Nanotechnol. **8**(7), 497–501 (2013).
[2]J. S. Ross, P. Klement, A. M. Jones, N. J. Ghimire, J. Yan, D. G. Mandrus, T. Taniguchi, K. Watanabe, K. Kitamura, W. Yao, D. H. Cobden, and X. Xu, Nat. Nanotechnol. **9**(4), 268–272 (2014).
[3]F. Withers, O. Del Pozo-Zamudio, A. Mishchenko, A. P. Rooney, A. Gholinia, K. Watanabe, T. Taniguchi, S. J. Haigh, A. K. Geim, A. I. Tartakovskii, and K. S. Novoselov, Nat. Mater. **14**(3), 301–306 (2015).
[4]T. Georgiou, R. Jalil, B. D. Belle, L. Britnell, R. V. Gorbachev, S. V. Morozov, Y. J. Kim, A. Gholinia, S. J. Haigh, O. Makarovsky, L. Eaves, L. A. Ponomarenko, A. K. Geim, K. S. Novoselov, and A. Mishchenko, Nat. Nanotechnol. **8**(2), 100–103 (2013).
[5]A. Splendiani, L. Sun, Y. Zhang, T. Li, J. Kim, C. Y. Chim, G. Galli, and F. Wang, Nano Lett. **10**(4), 1271–1275 (2010).
[6]K. F. Mak, C. Lee, J. Hone, J. Shan, and T. F. Heinz, "Atomically thin MoS_2: A new direct-gap semiconductor," Phys. Rev. Lett. **105**(13), 2–5 (2010).
[7]D. Y. Qiu, F. H. Da Jornada, and S. G. Louie, Phys. Rev. Lett. **111**(21), 1–5 (2013).
[8]A. Chernikov, T. C. Berkelbach, H. M. Hill, A. Rigosi, Y. Li, O. B. Aslan, D. R. Reichman, M. S. Hybertsen, and T. F. Heinz, Phys. Rev. Lett. **113**(7), 1–5 (2014).
[9]X. Liu, T. Galfsky, Z. Sun, F. Xia, E. C. Lin, Y. H. Lee, S. Kéna-Cohen, and V. M. Menon, Nat. Photonics **9**(1), 30–34 (2014).
[10]Z. Sun, J. Gu, A. Ghazaryan, Z. Shotan, C. R. Considine, M. Dollar, B. Chakraborty, X. Liu, P. Ghaemi, S. Kéna-Cohen, and V. M. Menon, Nat. Photonics **11**(8), 491–496 (2017).
[11]S. Dufferwiel, S. Schwarz, F. Withers, A. A. P. Trichet, F. Li, M. Sich, O. Del Pozo-Zamudio, C. Clark, A. Nalitov, D. D. Solnyshkov, G. Malpuech, K. S. Novoselov, J. M. Smith, M. S. Skolnick, D. N. Krizhanovskii, and A. I. Tartakovskii, Nat. Commun. **6**, 1–7 (2015).
[12]M. E. Kleemann, R. Chikkaraddy, E. M. Alexeev, D. Kos, C. Carnegie, W. Deacon, A. C. De Pury, C. Große, B. De Nijs, J. Mertens, A. I. Tartakovskii, and J. J. Baumberg, Nat. Commun. **8**(1), 1–7 (2017).
[13]S. Dufferwiel, T. P. Lyons, D. D. Solnyshkov, A. A. P. Trichet, A. Catanzaro, F. Withers, G. Malpuech, J. M. Smith, K. S. Novoselov, M. S. Skolnick, D. N. Krizhanovskii, and A. I. Tartakovskii, Nat. Commun. **9**(1), 4797 (2018).
[14]D. M. Myers, S. Mukherjee, J. Beaumariage, D. W. Snoke, M. Steger, L. N. Pfeiffer, and K. West, Phys. Rev. B **98**, 235302 (2018).
[15]H. J. Conley, B. Wang, J. I. Ziegler, R. F. Haglund, S. T. Pantelides, and K. I. Bolotin, Nano Lett. **13**(8), 3626–3630 (2013).
[16]K. He, C. Poole, K. F. Mak, and J. Shan, Nano Lett. **13**(6), 2931–2936 (2013).
[17]C. R. Zhu, G. Wang, B. L. Liu, X. Marie, X. F. Qiao, X. Zhang, X. X. Wu, H. Fan, P. H. Tan, T. Amand, and B. Urbaszek, Phys. Rev. B **88**(12), 1–5 (2013).
[18]Z. Sun, J. Beaumariage, H. C. P. Movva, S. Chowdhury, A. Roy, S. K. Banerjee, and D. W. Snoke, Solid State Commun. **288**, 18–21 (2019).
[19]W. Zefang, C. Yi-Hsin, H. Kevin, M. K. Fai, and S. Jie, Nano Lett. **1**(18), 137–143 (2018).
[20]C. Alberto, U. Dmitrii, A. Ahmet, W. Kenji, T. Takashi, and K. Andras, Nat. Photonics **13**, 131–136 (2019).
[21]L. S. R. Cavalcante, D. R. da Costa, G. A. Farias, D. R. Reichman, and A. Chaves, Phys. Rev. B **98**, 245309 (2018).
[22]B. Chakraborty, J. Gu, Z. Sun, M. Khatoniar, R. Bushati, A. L. Boehmke, R. Koots, and V. M. Menon, Nano Lett. **18**(10), 6455–6460 (2018).
[23]W. H. Chae, J. D. Cain, E. D. Hanson, A. A. Murthy, and V. P. Dravid, Appl. Phys. Lett. **111**(14), 143106 (2017).
[24]E. Del Corro, H. Terrones, A. Elias, C. Fantini, S. Feng, M. A. Nguyen, T. E. Mallouk, M. Terrones, and M. A. Pimenta, ACS Nano **8**(9), 9629–9635 (2014).
[25]A. Raja, A. Chaves, J. Yu, G. Arefe, H. M. Hill, A. F. Rigosi, T. C. Berkelbach, P. Nagler, C. Schüller, T. Korn, C. Nuckolls, J. Hone, L. E. Brus, T. F. Heinz, D. R. Reichman, and A. Chernikov, Nat. Commun. **8**, 1–7 (2017).
[26]D. J. Late, B. Liu, H. S. S. Ramakrishna Matte, V. P. Dravid, and C. N. R. Rao, ACS Nano **6**(6), 5635–5641 (2012).
[27]E. N. Esfahani, T. Li, B. Huang, X. Xu, and J. Li, Nano Energy **52**, 117–122 (2013).
[28]M. M. Alyörük, Y. Aierken, D. Çakır, F. M. Peeters, and C. Sevik, J. Phys. Chem. C **119**, 23231–23237 (2018).
[29]A. Islam and P. X.-L. Feng, J. Appl. Phys. **122**(8), 085704 (2017).
[30]S. Das and J. Appenzeller, Appl. Phys. Lett. **103**(10), 103501 (2013).
[31]J. Liang, K. Xu, B. Toncini, B. Bersch, B. Jariwala, Y.-C. Lin, J. Robinson, and S. K. Fullerton-Shirey, Adv. Mater. Interfaces **6**(3), 1801321 (2019).